Agricultural and Forest Meteorology 248 (2018) 372–385

Contents lists available at ScienceDirect

Agricultural and Forest Meteorology

journal homepage: www.elsevier.com/locate/agrformet

Research Paper

Water and energy fluxes over northern prairies as affected by chinook winds and winter precipitation

Matthew K. MacDonald[a,*], John W. Pomeroy[b], Richard L.H. Essery[a]

[a] School of GeoSciences, University of Edinburgh, King's Buildings, West Mains Road, Edinburgh, EH9 3JN, United Kingdom
[b] Centre for Hydrology, University of Saskatchewan, 117 Science Place, Saskatoon, SK, S7N 5C8, Canada

ARTICLE INFO

Keywords:
Latent heat
Sublimation
Evaporation
Snow
Eddy covariance
Hydrology

ABSTRACT

Chinooks are the North American variety of foehn: strong, warm and dry winds that descend lee mountain slopes. The strong wind speeds, high temperatures and substantial humidity deficits have been hypothesized to remove important prairie near-surface water storage from agricultural fields via evaporation, sublimation and blowing snow, as well as change the phase of near surface water via snowmelt and ground thaw. This paper presents observations of surface energy and water balances from eddy covariance instrumentation deployed at three open sites in southern Alberta, Canada during winter 2011–2012. Energy balances, snow and soil moisture budgets of three select chinook events were analysed in detail. These three events ranged in duration from two to nine days, and are representative of winter through early spring chinooks. Precipitation data from gauges and reanalyses (CaPA and ERA-interim) were used to assess water balances. Variations in precipitation and snowpacks caused the greatest differences in energy and water balances. Cumulative winter precipitation varied by a factor of two over the three sites: heaviest at the more northern site immediately east of the Rocky Mountains and lightest at the easternmost and southernmost site. The temporal progression of chinook-driven surface water loss is explained, beginning with strong blowing snow events through to evaporation of meltwater as snowpacks disappear. At the two sites with considerable winter precipitation and snowcover, large upward latent heat fluxes, often exceeding 100 W m^{-2}, were driven by downward sensible heat fluxes but were unrelated to net radiation. Conversely, at the southernmost site with little snowcover, upward latent heat fluxes were much smaller (less than 50 W m^{-2}) and were associated with periods of positive net radiation. Upward sensible heat fluxes during periods of positive net radiation were observed at this site throughout winter, but were not observed at the more northerly sites until March when the snowcovers ablated. Daily sublimation plus evaporation rates during chinooks at the sites with heaviest and lightest precipitation were 1.3–2.1 mm/day and 0.1–0.3 mm/day, respectively. Evaporation of soil water occurred while soils were partially to fully unfrozen in November. There was little change in soil water content between fall freeze-up and spring thaw (December through most of March), indicating that over-winter infiltration was balanced by soil water evaporation and both terms were likely to be small. Winter precipitation resulted in only 2% to 4% increases in near-surface water storage at the more northern sites with greater precipitation, whereas there was a net loss over winter at the southernmost site.

1. Introduction

Chinooks are the North American variety of foehn: strong, warm and dry westerly winds that descend lee mountain slopes as a result of synoptically driven flow (AMS, 2012). They occur east of the Rocky Mountains, extending from Central Alberta southward to New Mexico. Chinooks result in strong winds, high temperatures and humidity deficits that can significantly alter the storage and transfer of water during winter. The hydrology of the semi-arid prairies of southern Alberta, Canada can be highly sensitive to the frequency and severity of chinooks as runoff generation largely depends on spring snowmelt rates exceeding infiltration rates into frozen soils (Steed, 1982; Gray et al., 1986; Nkemdirim, 1991).

Chinooks create notable meteorological contrast to the cold, high pressure Arctic air mass that is confined east of Rocky Mountains over the prairies of southern Alberta. Chinooks are generated from strong synoptic pressure gradients over the eastern Pacific Ocean that direct warm air eastward. They occur throughout the year but their impacts

* Corresponding author. Present address: Department of Civil Engineering, University of Manitoba, E1-368 EITC, 15 Gillson St., Winnipeg, MB, R3T 5V6, Canada.
E-mail address: matthew.macdonald@umanitoba.ca (M.K. MacDonald).

http://dx.doi.org/10.1016/j.agrformet.2017.10.025
Received 2 February 2017; Received in revised form 16 October 2017; Accepted 18 October 2017
Available online 20 October 2017

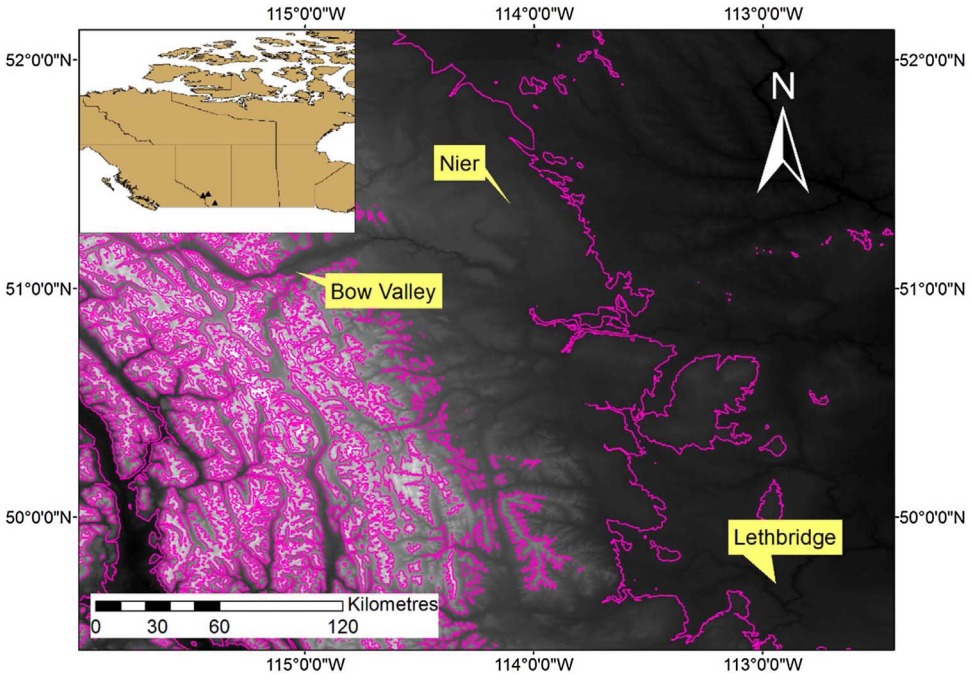

Fig. 1. Locations of experimental sites. Inset shows site locations in western Canada. Purple lines are 500 m elevation contours.

are most noticeable during winter when they result in strong winds and unseasonably warm temperature across southern Alberta (Nkemdirim, 1996).

Nkemdirim (1991, 1996, 1997), described aspects of the climatology of chinooks in Alberta. The following criteria were used to identify chinook events in Calgary from hourly station observations for November through February between 1951 and 1990 (Nkemdirim, 1991): (i) sustained westerly winds between the SSW and WNW directions, (ii) wind speed exceeding 4.5 m/s, (iii) sharp increase in temperature with daily mean exceeding the historical normal value, (iv) decrease in relative humidity, and (v) the increase in temperature and decrease in relative humidity correlate perfectly with the shift to westerly winds. On average there are 50 days from November through February in Calgary with chinook events (standard deviation of 16 days). December has the greatest number of chinook days (14.5), and February the least (11). Durations of chinook events range from 1 to 17 days, though single day chinooks are most common (Nkemdirim, 1997). Incoming shortwave and longwave radiation are on average 12 W m^{-2} and 27 W m^{-2} greater during Chinook than non-chinook conditions (Nkemdirim, 1990; Nkemdirim, 1995). Increased warming during chinooks generally occurs from north to south and from west to east, and at lower elevations (Nkemdirim, 1996).

Chinooks can alter the water balance via snowmelt, sublimation, blowing snow transport, ground thaw and evaporation. Steed (1982) estimated that the seasonal snow mass in southern Alberta is depleted by over 50% by chinooks. Studies have provided estimates of high sublimation rates during chinook conditions in alpine regions in the western USA: over 2 mm/day (Cline, 1997), 0.5 mm/day (Hood et al., 1999), 3–4 mm/day (Leydecker and Melack, 1999). Golding (1978) estimated potential sublimation during chinooks over a number of alpine and subalpine sites along the eastern slopes of the Rocky Mountains in Alberta and found average values of 1.2–2.0 mm/day, which exceeded snowmelt during these events. These estimates could have included sublimation of blowing snow, which MacDonald et al. (2010), Fang et al. (2013) and Musselman et al. (2015) found to be substantial at the same site. Hayashi et al. (2005) observed sublimation rates up to 2.2 mm/day associated with foehn-type winds during the snowmelt period over an agricultural field in northern Japan. Nkemdirim (1991) studied evaporation during chinooks in Calgary and found evaporation near the potential rate when snowmelt results in standing water and shallow soil moisture is saturated and unfrozen. Of the aforementioned studies, only Nkemdirim (1991) presents energy balance results from a prairie site in Alberta; this was from a single station located within the urban area of Calgary and only bulk estimates of turbulent fluxes were presented.

A number of field studies have characterised Canadian Prairie winter hydrological processes, but most were located in Saskatchewan which is east of the area most heavily affected by chinooks. Prairie snowmelt in Saskatchewan occurs in March or April and is primarily driven by solar radiation (Gray et al., 1986). Sublimation losses are low (0.2 mm per day maximum) in this region (Granger and Male, 1978). Blowing snow wind erosion is a significant ablation processes in the prairies, particularly east of the chinook region where snowpacks remain cold throughout winter (Pomeroy et al., 1993; Pomeroy and Li, 2000; Fang and Pomeroy, 2009). Blowing snow involves the redistribution of snow mass, and enhanced sublimation rates compared to that from static snowpacks. Blowing snow sublimation losses of 15%–41% of annual snowfall have been estimated for the Canadian Prairies (Pomeroy and Gray, 1995). Pomeroy and Essery (1999) observed upward latent heat fluxes of 40–60 W m^{-2} during mid-winter blowing snow events; which are considerably greater than those observed over melting prairie snowpacks during periods of high net radiation. Infiltration of meltwater into frozen soils during winter can be restricted completely when surficial soils are saturated and frozen (Gray et al., 1985a). Shallow soil moisture content usually decreases over winter, and both liquid and vapour soil moisture transport mechanisms can be important (Gray et al., 1985b).

This paper presents direct measurements of water and energy balance components from three sites located in the prairies of southern Alberta over winter 2011–2012. The objectives of this study are to characterize the spatial variability of 1) surface energy and water fluxes during chinooks, and 2) winter season changes in surface and shallow sub-surface water storage. Time series of selected chinooks events are analysed in detail. Lastly, the winter season water balance components at each site are assessed using different sources of precipitation data.

Table 1
Instruments used in this study at (a) Bow Valley, (b) Nier and (c) Lethbridge.

(a)

Variable	Instrument	Height(s) or depths(s)
Air temperature/humidity	Campbell Scientific HMP45C capacitance hygrometer and thermistor (2)	0.40, 1.28, 2.04 m
Wind speed	Met One 014A 3-cup anemometer (2)	0.46, 5.3 m
Wind fluctuations	Campbell Scientific CSAT3 ultrasonic anemometer	2.03 m
Vapour fluctuations	Campbell Scientific KH2O hygrometer	2.03 m
Radiation (incoming/outgoing shortwave & longwave)	Kipp & Zonen CNR4 pyrgeometer and pyranometer	1.88 m
Snow depth	Campbell Scientific SR50A ultrasonic snow depth gauge	1.68 m
Soil moisture	Campbell Scientific CS616 water content reflectometer (3)	0.02–0.025, 0.055–0.085, 0.185–0.215 m
Soil temperature	Type-T thermocouple wire (3)	0.023, 0.07, 0.20 m
Ground heat flux	Hukseflux HFT1 heat flux plate (2)	0.01 m

(b)

Variable	Model	Height(s) or depths(s)
Air temperature/humidity	Campbell Scientific HMP45C capacitance hygrometer and thermistor (2)	0.95, 1.87 m
Wind speed[a]	Met One 014A 3-cup anemometer	2.0 m
	RM Young 05103 wind monitor	10.0 m
Wind fluctuations	Campbell Scientific CSAT3 ultrasonic anemometer	1.89 m
Vapour fluctuations	Campbell Scientific KH2O hygrometer	1.89 m
Radiation (incoming/outgoing shortwave & longwave)	Kipp & Zonen CNR1 pyrgeometer and pyranometer	1.84 m
Snow depth[a]	Campbell Scientific SR50 ultrasonic snow depth gauge	1.68 m
Soil moisture[a]	Campbell Scientific CS615 water content reflectometer (2)	0.05, 0.20 m
Soil temperature[a]	Type-T thermocouple wire (2)	0.05, 0.20 m
Ground heat flux	Hukseflux HFT1 heat flux plate	0.01 m

(c)

Variable	Model	Height(s) or depths(s)
Air temperature/humidity	Campbell Scientific HMP45 capacitance hygromete and thermistor.	1.0 m
Wind speed/direction[b]	RM Young ultrasonic anemometer	6.0 m
Wind fluctuations[b]	Solent 1012R3 ultrasonic anemometer	6.0 m
Gas analysis[b]	LiCor LI-6262 CO_2/H_2O analyzer	6.0 m
Net radiation[b]	REBS Q*7.1 net radiometer	3.0 m
Surface temperature (outgoing longwave radiation)	Type-K thermocouple wire	1.3 m
Soil moisture[b]	Campbell Scientific CS615 water content reflectometer (1 × 4,2 × 2)	0.00–0.15 (4), 0.15 (2), 0.30 (2) m
Soil temperature[b]	thermocouple wire (5 × 2)	0.02 (2), 0.04 (2), 0.08 (2), 0.16 (2), 0.32 (2) m
Ground heat flux[b]	REBS HFT-3.1 heat flux plate (4)	0.02 m
Atmospheric pressure[b]	Vaisala PTB01 analogue barometer	–

[a] indicates instruments operated by Alberta Agriculture and Rural Development.
[b] indicates instruments operated by L.B. Flanagan, University of Lethbridge.

2. Methods

2.1. Experimental sites

Instruments consisting of eddy covariance, net radiation and soil heat flux systems were installed at three sites in southern Alberta, east of the Rocky Mountains (Fig. 1; Table 1). These three locations, ranging 215 km north-south and 175 km east-west, were selected to span the area most affected by chinooks (Nkemdirim, 1996). The observation period was November 2011 through early-April 2012. Soils at each site are predominantly mineral with surficial soils being over 80% sand and silt (Table 2).

2.1.1. Bow Valley

The Bow Valley (BV) instrumentation was located in a large clearing within a coniferous forest, along the eastern periphery of the Rocky Mountains (51° 04′ 10″ N, 115° 02′ 49″ W; 1326 m ASL). It was the most western of the three sites and nearest the mountains. Instruments were mounted on a 5 m triangular tower and the sonic anemometer was oriented SSW to capture chinook events, with an upwind fetch of 230 m to the forest edge. Manual snow surveys of 36 depth measurements at 5-m intervals and five density measurements using a Perla-type RIP volumetric snow cutter were conducted twenty times from December through March. Vegetation cover was mostly grass 1–10 cm in height, with a mean height of approximately 5 cm. The field had sparsely

Table 2
Soil information for experimental sites (Soil Landscapes of Canada Working Group, 2010).

	Bow Valley (cm depth)			Nier (cm depth)			Lethbridge (cm depth)		
	0–10	20–35	51–70	0–20	0–35	0–100	15–20	0–100	58–100
Sand (%)	40	31	32	40	43	40	43	40	25
Silt (%)	40	44	33	40	39	30	29	30	40
Clay (%)	20	25	35	20	18	30	28	30	35
Organic (%)	3.9	2.1	0.0	5.0	5.2	1.0	1.3	1.0	0.0
Bulk density (g cm^{-3})	1.15	1.40	1.45	1.20	1.15	1.15	1.15	1.15	1.15

spaced shrubs, approximately 7 shrubs per 100 m^2 in the upwind direction. These shrubs ranged in height from 15 to 40 cm, with a mean height of 28 cm. The mean shrub width was approximately 17 cm, being widest at mid-height. The vegetation was dormant during the study period. Atmospheric pressure data from a nearby Environment Canada station were used (2.0 km to the north-northwest of BV; 1293 m ASL).

2.1.2. Nier

The Nier site is an Alberta Ministry of Agriculture and Rural Development (AARD) meteorological station located in a cultivated prairie field in central Alberta (51° 22′ 09″ N, 114° 05′ 58″ W; 1145 m ASL), and was the northernmost of the three sites. Upwind fetch was approximately 500 m to sparse trees and a narrow, heavily-incised creek. A 2 m triangular tower was set-up within the existing instrumentation compound, and additional instruments were installed. Manual snow surveys were performed, consisting of 40 depth measurements at 5 m intervals and five density measurements using a Perla-type RIP volumetric snow cutter. Twelve snow surveys were conducted from December through March. The field was covered by tall grass, much of which was lying horizontally along the ground surface. The height of bent-over grass was 2–25 cm, with a mean height of 7 cm. The height of the erect grass was 7–48 cm, with a mean height of 27 cm. The overall mean grass height was 12 cm. Pressure data from the Calgary International Airport (29 km to the south) was used.

2.1.3. Lethbridge

The Lethbridge site is an AmeriFlux site operated by Dr. Larry Flanagan, University of Lethbridge Department of Biological Sciences, with detailed information found in Flanagan et al. (2002) and Flanagan and Adkinson (2011). It is located over grassland in southern Alberta (49° 25′ 48″ N, 112° 33′ 36″ W; 951 m ASL), and is the southernmost of the three sites. The sonic anemometer is oriented to the west, with an upwind fetch greater than 600 m. Mean grass height was 18.5 ± 3.5 cm standard deviation. A time-lapse digital webcam was operated at the Lethbridge site from 7 December 2011 as part of the Phenocam network (Richardson et al., 2007), and was used to qualitatively describe snowcover. Snow surveys were not performed at this site.

2.2. Flux data processing and gap filling

For BV and Nier, high frequency eddy covariance data were collected at 20 Hz and processed using the EdiRe software package (http://www.geos.ed.ac.uk/homes/jbm/micromet/EdiRe/). The high frequency BV data was subject to a regular AC power electrical interference resulting in removal of 15% of data.

Raw high frequency data were quality checked before performing corrections and time-averaging following procedures outlined by Vickers and Mahrt (1997): despiking, checks for anomalously large or small values of skewness and kurtosis, ogives procedure to determine appropriate block averaging periods (determined to be 30 min), and flux stationarity test (Foken and Wichura, 1996). For BV, planar fit coordinate rotation (Wilczak et al., 2001) was performed. For Nier, coordinate rotation was undertaken using the standard technique of adjusting the mean vertical wind components to zero because much of northerly and easterly flow was distorted by other instruments and masts, preventing the calculation of a plane surface. Other standard corrections were applied: frequency response (Moore, 1986) using the co-spectral models of Kaimal et al. (1972, 1976) and air density (Webb et al., 1980). Similar flux averaging and corrections were performed for the Lethbridge data, as detailed in Flanagan et al. (2002) and, Flanagan and Adkinson (2011).

The energy balance closure analyses were restricted to cold periods when snowcover was complete, or when no snow was present, to reduce uncertainty associated with estimating phase change and local advection over patchy snowcover. Snowpack heat storage was neglected because of the difficulty in obtaining temperature measurements within shallow snowpacks and avoiding assuming snow density. The convention of non-radiative fluxes (sensible heat flux [H], latent heat flux [λE] and ground heat flux [G]) being positive away from the surface is used. Linear regression of $H + \lambda E$ against $Q^* - G - \Delta Q_S$ is shown, where Q^* is net radiation and ΔQ_S is the sum of below-sensor air-space sensible and latent heat storage (e.g. Leuning et al., 2012; Chen et al., 2011). ΔQ_S values were low, near 1 W m^{-2} at most times. Soil heat storage was neglected because the heat flux plates were placed 1 cm below the surface. Negligible soil temperature changes would have occurred below snowcover, but it is possible that small energy storage changes were missed during bare conditions. A perfect linear regression of energy balance closure has a slope (energy balance ratio) of one and an intercept of zero. Turbulent fluxes are normally underestimated and energy imbalances are expected (Kelliher et al., 1997; Constantin et al., 1998; Ohta et al., 2001). A FLUXNET study encompassing many sites and years of data (Wilson et al., 2002) resulted in energy balance ratios of 0.53–0.99, with a mean slope of 0.79. The slopes at the BV and Nier sites are at the low end of the range presented in the aforementioned FLUXNET study meaning an undermeasurement of net turbulent fluxes or missing energy balance terms (Table 3). The energy balance ratio at Lethbridge over the study period was slightly better than at BV and Nier. Energy balance closure at all sites would likely be improved if all phase change and storage terms were measured. It is not believed that the use of both open- and closed-path water vapour sensor effects the conclusions presented in this paper (Haslwanter et al., 2009).

Recent observations have shown that there remain difficulties in closing energy balances of snowpacks even during ideal conditions (i.e. homogeneous surface, relatively flat and extensive) and that neither internal snowpack energetics nor atmospheric exchanges are fully understood. Helgason and Pomeroy (2012a) observed a persistent longwave cooling over a homogeneous prairie snowpack, which was not offset by other measured fluxes. They suggest that an unmeasured exchange of sensible heat is the culprit of the energy imbalance. Furthermore, in mountain valley bottoms, there is additional advected turbulence associated with mountain topography and other land surface discontinuities (i.e. additional stress from outside internal boundary layers; Helgason and Pomeroy, 2012b). To account for uncertainty in instrumental underestimation of fluxes and potential for systematic error in the gap-filling procedure (e.g. flux divergence, nonstationary flow, advection, high-frequency spectral losses and poor sampling of the largest eddies), it was estimated that λE could have been 10% greater than observed. This value is based on error estimates from the EBEX- 2000 and LITFASS-2003 experiments (Mauder et al., 2006) and for CSAT3 sonic anemometers (Foken and Oncley, 1995; Foken, 2008).

Gaps in E (evaporation in mm) were filled with the average of adjacent values if 120 min or less were missing. Gaps greater than 120 min were filled using the bulk aerodynamic formulation for moisture with the β (water availability factor) parameterization of water availability, given by:

$$E = \beta \rho C_q \overline{u} \{q_{sat}(T_0) - q_z\} \quad (1)$$

Table 3
Linear regression of energy balance closure for experimental flux sites.

Site	Number of observations	Slope [energy balance ratio]	Intercept (W m^{-2})	R^2	Mean residual (W m^{-2})
Bow Valley	3186	0.59	0.34	0.78	23.1
Nier	1585	0.65	2.20	0.88	36.5
Lethbridge	1867	0.72	−2.37	0.89	18.9

Table 4
Precipitation gauges.

Experimental site	Precipitation site	Operator	Distance and direction from experimental site	Gauge type
Bow Valley 51°04′10" N, 115°02′49" W; 1326 m ASL	Bow Valley	Environment Canada	2.0 km (NW)	Alter-shielded Geonor
Nier 51°22′09" N, 114°05′58" W; 1145 m ASL	Nier	Alberta Agriculture & Rural Development	–	Alter-shielded Geonor
Lethbridge 49°25′48" N, 112°33′36" W; 951 m ASL	Demo Farm	Alberta Agriculture & Rural Development	14.9 km (NW)	Alter-shielded Geonor

Table 5
Mean values of meteorological variables for chinook vs. non-chinook periods over winter 2011–2012. Statistically significant different mean values are shown in bold (*t*-test; $p < 0.01$; all variables pass the Shapiro–Wilk test for normality).

Site	u* (m/s)		q (10^{-3} kg/kg)		T (°C)		Q* (W/m^2)		H (W/m^2)		λE (W/m^2)	
	Chin	Non	Chin	Non	Chin	Non	Chin	Non	Chin	Non	Chin	Non
BV	0.38	0.18	3.0	3.6	0.7	−8.7	4.7	10.6	−33.5	−1.7	38.1	4.6
Nier	0.33	0.25	3.1	3.3	−0.1	−9.5	−2.9	0.9	−21.7	−5.1	23.3	6.2
Leth	0.47	0.24	2.3	2.0	1.7	−6.3	−8.5	0.4	−15.4	8.4	4.0	1.8

Table 6
Climate normals (1981–2010) for experimental sites compared to winter 2011–2012.

Experimental site	Climate normal site and distance from experimental site	Mean November-March temperature (°C)		November-March Precipitation (mm)	
		Normal	2011–2012	Normal	2011–2012
Bow Valley	Kananaskis, 4.7 km S; 1391 m ASL	−4.7	−2.6	159.1	184.6
Nier	Calgary Airport, 28.9 km S; 1084 m ASL	−5.5	−2.6	62.3	65.9
Lethbridge	Lethbridge Airport, 19.5 km NW; 929 m ASL	−4.0	−1.5	86.8	17.7

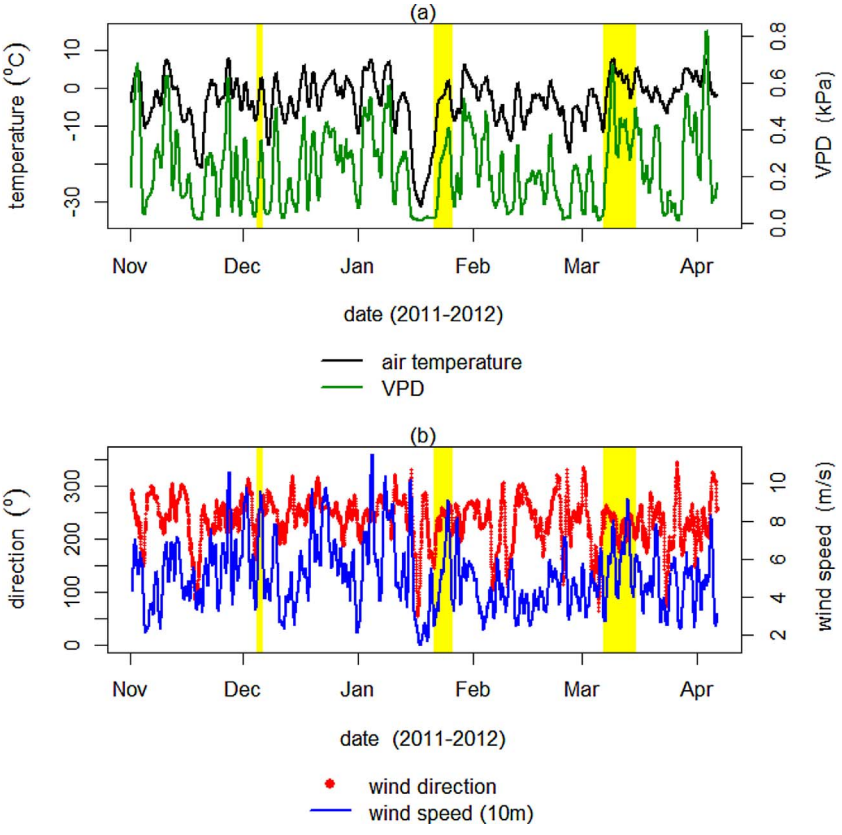

Fig. 2. Surface meteorology at Nier during the study period showing (a) temperature and vapour pressure deficit (VPD), and (b) wind speed and direction. Chinook periods selected for analyses are highlighted in yellow. Temperature, VPD and wind speed are plotted as 24-h moving averages and direction every 6 h is plotted.

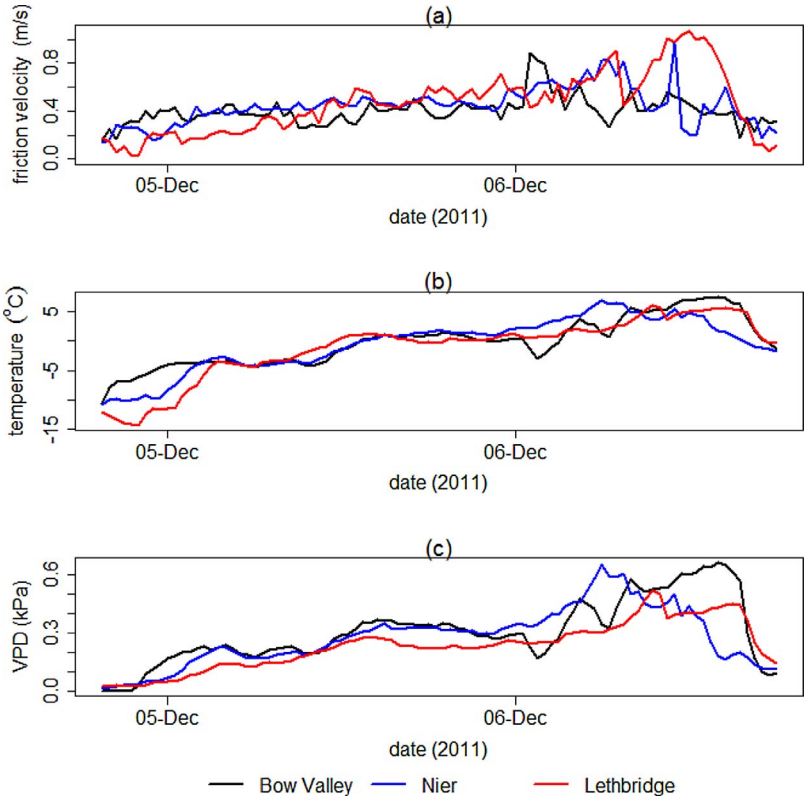

Fig. 3. Surface meteorology at all sites for 4–6 December 2011: (a) friction velocity (u*), (b) air temperature, and (c) vapour pressure deficit.

where ρ is air density, C_q is the transfer coefficient for moisture, $\overline{u}$ is the mean horizontal wind speed, q_{sat} is the saturation specific humidity at the observed surface temperature T_0, q_z is the specific humidity at instrument height z. E derived from the eddy covariance observations were used in Eq. (1) to back-calculate the term βC_q. Gap-filled E accounted for 18%, 34% and 16% of data at BV, Nier and Lethbridge, respectively.

2.3. Precipitation

Precipitation from both gauges and reanalyses were considered in assessing water balances. Snowfall observations from Geonor gauges (Table 4) were corrected for undercatch due to wind following Smith (2009). Precipitation from two reanalysis datasets were also used due to uncertainty of the gauge undercatch correction: the Canadian Precipitation Analysis (CaPA; Mahfouf et al., 2007) and the European Centre for Medium Range Weather Forecasts (ECMWF) Re-analysis (ERA-interim; Dee et al., 2011). These reanalyses were also assessed for the potential of future large-scale modelling over the region.

2.4. Soil moisture

2.4.1. Soil unfrozen water content

Soils were partially frozen throughout the study period. Below freezing, water molecules nearest soil particles remain in liquid form due to absorptive and capillary forces. Time-domain reflectometry does not measure frozen water content, making it difficult to determine whether observed increases in soil liquid water content (LWC) were due to infiltration or were strictly due to soil thaw. Soil freezing curves were calculated to ascertain whether changes in LWC in partially frozen soils were due to phase change. The equation relating water suction to soil temperature when ice is present (Miller, 1965; Black and Tice, 1988) is combined with the Clapp and Hornberger (1978) equation for suction as a function of LWC to give the upper limit of liquid water content for subfreezing temperatures:

$$\Theta_l^{max} = \Theta_s\left(-\frac{\kappa T}{\Psi_s}\right)^{-1/b} \quad (2)$$

where Θ_l^{max} is the maximum volumetric liquid water content at temperature T, Θ_s is the saturation volumetric soil water content, $\kappa = 114.3\ \mathrm{m\ K^{-1}}$ is a constant, Ψ_s is the saturation water suction, and b is a soil texture specific constant. Values for Θ_s, Ψ_s and b were derived for each site using the empirical relationships presented by Cosby et al. (1984) and site soil texture data. Equation [2] has been used in several studies (e.g. Fuchs et al., 1978; Flerchinger and Saxton, 1989; Zhao and Gray, 1997).

2.4.2. Soil water mass

Unfrozen soil water mass to 35 cm depth was calculated at each site by depth averaging volumetric moisture measurements (Table 1). It is unlikely that a single set of water content measurements is representative of the mean soil moisture of the field or footprint of the eddy covariance system. Equations from Famiglietti et al. (2008) in terms of mean soil moisture content for the standard deviation of soil moisture at the 100 m scale were used to quantify uncertainty in soil water mass. These relationships were developed using observations from four intensive observation campaigns (the Southern Great Plains Hydrology Experiments 1997 and 1999, and the Soil Moisture Experiments 2002 and 2003). It was assumed that the true field mean soil moisture is within the observed value ± 1 standard deviation.

2.5. Blowing snow modelling

Blowing snow transport was an unobserved water balance term, though blowing snow events during chinooks were visually identified and common at the BV and Nier sites. Snow transport estimates were obtained by linking the Prairie Blowing Snow Model (PBSM; Pomeroy et al., 1993; Pomeroy and Li, 2000) with the Energy Budget Snowmelt Model (EBSM; Gray and Landine, 1988) and applied in single column mode at each site.

PBSM was developed for application over the Canadian Prairies, and

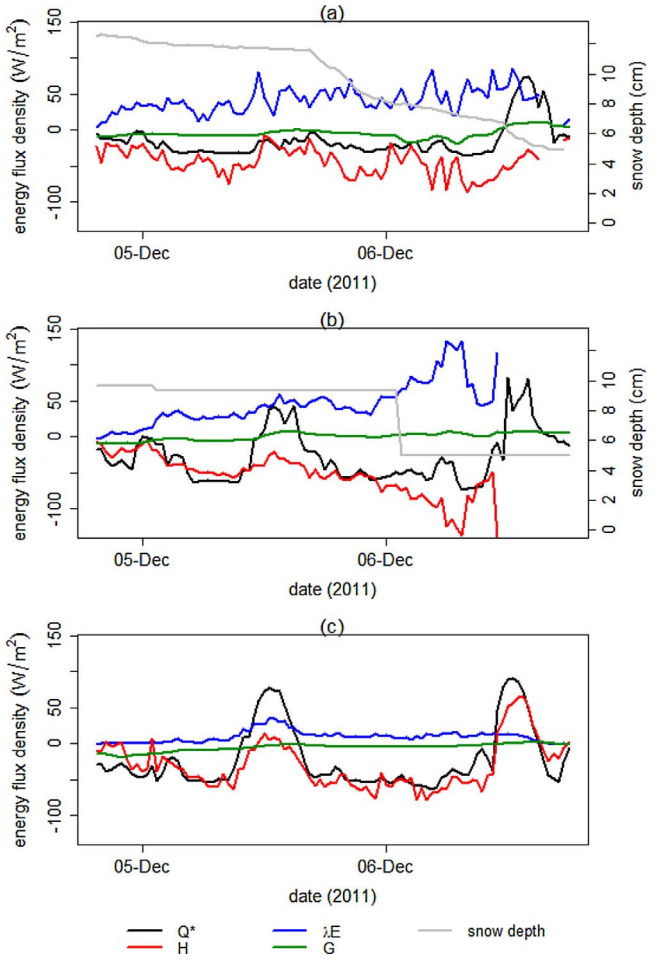

Fig. 4. Energy fluxes and snow depth for 4–6 December 2011 at (a) Bow Valley, (b) Nier, and (c) Lethbridge. Snow depth is not shown for Lethbridge because the initial depth was only 1 cm and measurements were degraded by vegetation.

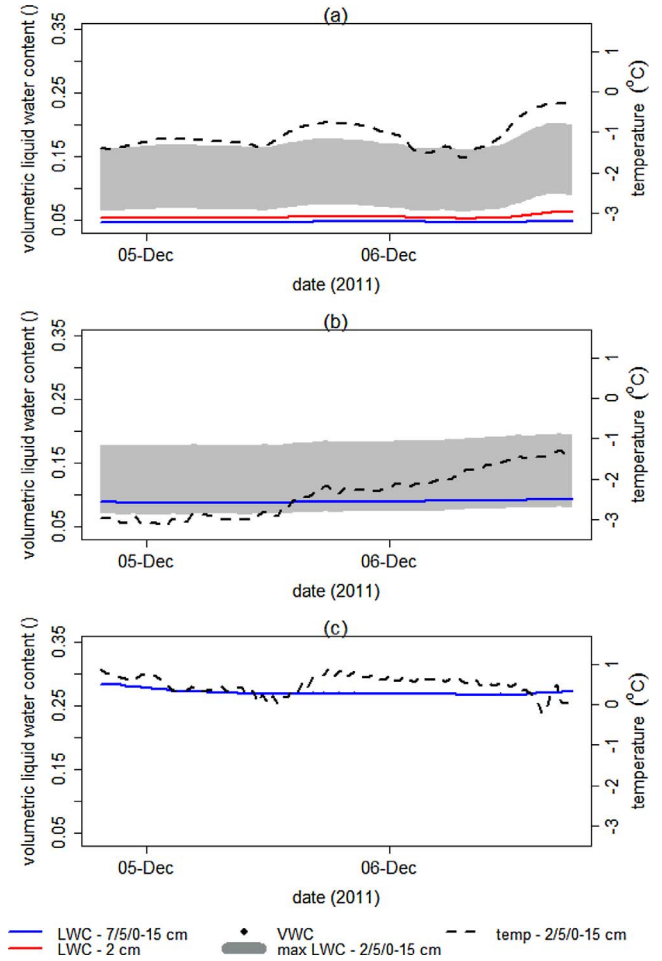

Fig. 5. Soil temperature, observed liquid water content (LWC) and calculated maximum LWC for 4–6 December 2011 at (a) Bow Valley, (b) Nier, and (c) Lethbridge. The range in calculated maximum in LWC is calculated using mean hydraulic parameter values ± 1 standard deviation.

calculates one-dimensional blowing snow transport and sublimation rates for steady-state conditions up to a boundary layer height determined by upwind fetch and wind speed (Pomeroy et al., 1993). A range of snow transport quantities were estimated for each site by varying the vegetation height from its mean observed value ± 3 cm: 2–8 cm at BV, 4–10 cm at Nier, and 15.5–21.5 cm at Lethbridge.

3. Results

3.1. Observations

Chinook identification criteria similar to Nkemdirim (1991, 1997) were used: concurrent sustained westerly winds increasing in speed, increasing air temperature and vapour pressure deficit (VPD). Nkemdirim's minimum wind speed criterion of 4.5 m s^{-1} was not used; rather, any increase in wind speed was accepted. The end-of-chinook criteria were opposite to chinook identification criteria: concurrent sustained northerly to easterly winds decreasing in speed, decreasing air temperature and VPD. It is difficult to specify the exact time of the beginning of a chinook; the occurrences of aforementioned criteria were rarely all coincident and occasionally occurred hours apart.

From a micrometeorological perspective, chinook and non-chinooks periods were notably different during winter 2011–2012 (Table 5). Mean wind speed (quantified as friction velocity [u*]), specific humidity, air temperature, Q*, H and λE were statistically significantly different ($p < 0.01$) between non-chinook and chinook periods at all sites, with the exception of Q* at Nier. Indeed chinooks brought higher wind speeds, air temperatures and humidity deficits, which in turned caused higher turbulent fluxes despite lower Q*. It is noted that winter 2011–2012 was over 2 °C warmer than the 1981–2010 climate normal period. Precipitation was heavier than normal at BV but much lighter than normal at Lethbridge (Table 6).

Three chinook events are highlighted: 4–6 December 2011, 21–26 January 2012 and 6–15 March 2012 (Fig. 2). These three periods were selected for completeness of flux observations and to highlight different periods during the winter. The 4–6 December event was a relatively brief chinook. The 6–15 March event is considered an early spring event when downwelling shortwave radiation was much larger than during mid-winter.

Snow depths from ultrasonic measurements are subsequently presented as well. Only daily average snow depth data were available for Nier, which explains the step changes in depth shown. Snow depth observations from Lethbridge were not used. Snow cover was very shallow at this site and readings were severely degraded by the presence of tall grass.

3.1.1. 4–6 December 2011

The onset of this chinook was at approximately the same time at BV and Lethbridge but later at Nier (Fig. 3). Air temperature and u* increased at BV and Lethbridge from approximately 22:00 on 4 December, whereas at Nier these variables did not increase until three to four hours later. There was a similar timing of increasing VPD at all sites, from both temperature increase and humidity decrease.

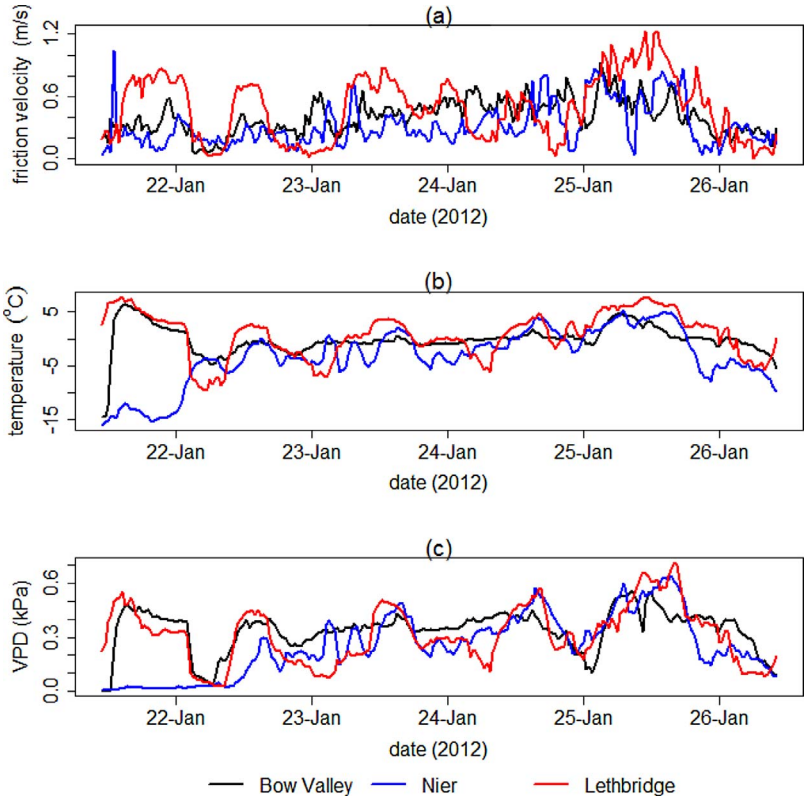

Fig. 6. Surface meteorology at all sites for 21–26 January 2012: (a) friction velocity (u*), (b) air temperature, and (c) vapour pressure deficit.

Snowcover was present initially at both BV and Nier, with the initial snowpack deeper at BV (Fig. 4). Most of the snow at both BV and Nier was eroded by blowing snow until the early morning of 6 December. Up until this time air temperatures were below or just above freezing and wind speeds were high (Fig. 3b), conditions suitable for blowing snow. 5 cm of snow depth (1.4 mm SWE from snow surveys) may have been eroded by wind at BV. It is more difficult to make a quantitative assessment at Nier because only daily snow depth data were available. The magnitudes of turbulent fluxes during this initial cold period with blowing snow were below 50 W m^{-2} at BV and Nier (Fig. 4). From 6 December, air temperatures were well above freezing at BV and Nier, and surface temperatures were near freezing (not shown) which indicates that snowmelt was likely occurring. The presence of liquid water results in greater cohesion amongst snow crystals within the snowpack, which restricts the occurrence of blowing snow (e.g. Li and Pomeroy, 1997). The magnitudes of turbulent fluxes during this period of wet snowpacks were greater at Nier than at BV and, at both sites, were greater than during the initial colder period with blowing snow. Precipitation observations indicate that a trace amount of snow was present initially at Lethbridge. Turbulent fluxes were smaller in magnitude at Lethbridge than at BV or Nier.

Q* remained negative for one to two days at BV and Nier until snowcovers became heterogeneous, resulting in a lower albedo (Fig. 4). Negative Q* cooled the surface which allowed surface downward H. Daytime Q* at Lethbridge was much greater as there was little snowcover. H was downward at both BV and Nier throughout this chinook, caused by the difference between air and surface potential temperatures. Conversely, H was upward at Lethbridge during periods with positive Q*. Downward H was driving upward λE at BV and Nier, whereas the peak λE at Lethbridge occurred during high Q*. The turbulent fluxes were the largest components of the energy balance at BV and Nier, whereas Q* was usually largest at Lethbridge. The increasing magnitude of turbulent fluxes, particularly at Nier, corresponded with increased air temperature and VPD (Fig. 3). Average daily evaporation + sublimation during this chinook was 1.30 mm/day at BV, 1.41 mm/day at Nier, and 0.32 mm/day at Lethbridge. G was low at all sites and associated with positive Q* during daytime.

Fig. 5 shows soil temperature and observed liquid water content (LWC) during this chinook. For clarity, only the near-surface observations are shown: 2 cm and 7 cm below ground surface at BV; 5 cm at Nier; 0–15 cm (mean) at Lethbridge. Soil temperatures were above freezing at Lethbridge, whereas they remained below freezing at both BV and Nier. Correspondently, the initial LWC at all depths was considerably greater at Lethbridge than at either Nier or BV. Changes in measured LWC were due to phase change, and there was no evidence of infiltration. These figures show observed LWC and theoretical maximum possible liquid water content (max LWC) in frozen soils calculated using Eq. (2). A range of freezing curves are shown, bounded by calculations using mean parameter values for Θ_s, Ψ_s and b ± one standard deviation (Cosby et al., 1984). Calculated changes in max LWC are only due to freezing and thawing resulting from changes in temperature. For instance, at BV, increases and decreases in LWC follow the temperature profile and correlate well with calculated changes in max LWC (Fig. 5a). Had infiltration occurred, the observed LWC would have increased more sharply than the theoretical max LWC. Soil temperature at 2 cm follows a diurnal pattern, increasing with positive Q*. Similarly, increasing LWC at 5 cm at Nier was due to increasing soil temperature (Fig. 5b). Soil temperatures at Lethbridge were above freezing, until the end of this chinook, thus all soil moisture was in liquid form.

3.1.2. 21–26 January 2012

This chinook occurred 10–11 h sooner at both BV and Lethbridge than at Nier, and was associated with sharp increases in temperature and VPD (Fig. 6). Initial snowcover was complete at both BV and Nier, with BV having the deeper snowpack (Fig. 7). Blowing snow likely occurred at BV through 24 January, as temperature was greater than 0 °C and wind speeds were high. Saltation was observed during a site visit to BV on 23 January, but on 25 January the snowpack was observed to be damp and static. Up to 6 cm of snow depth (approximately 5 mm SWE from snow surveys) was eroded by wind at BV. Snow

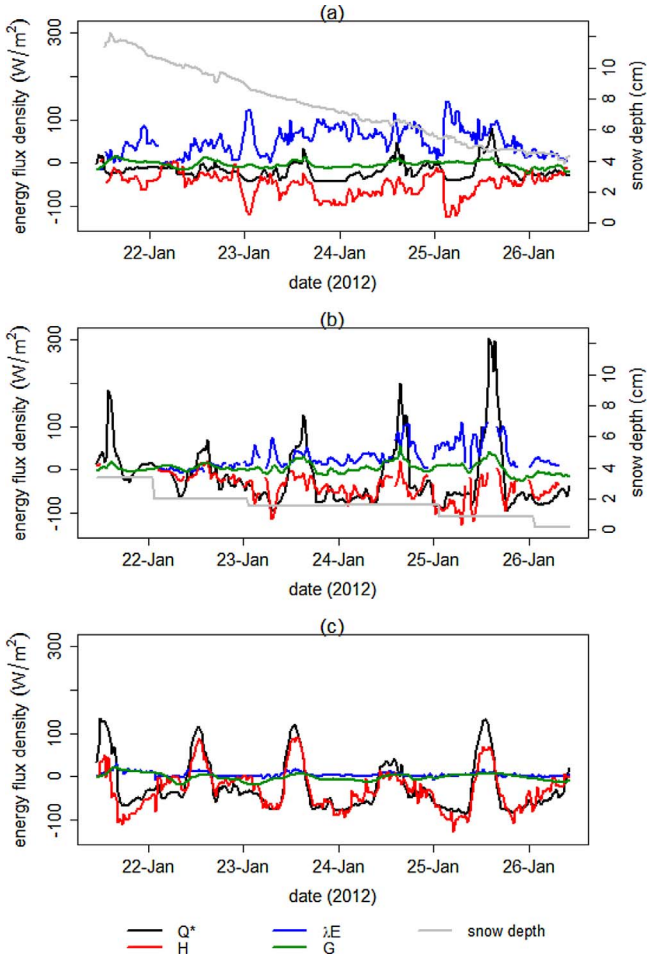

Fig. 7. Energy fluxes and snow depth for 21–26 January 2012 at (a) Bow Valley, (b) Nier, and (c) Lethbridge. Snow depth is not shown for Lethbridge because only a trace amount was initially present and measurements were degraded by vegetation.

erosion by wind likely occurred at Nier through 22 January, but thereafter the snowcover was shallow, wet and patchy. From the daily snow depth data, 1.8 cm of snow depth was eroded at Nier.

Q* was mostly negative at BV, and did not become positive until the snowpack warmed and more ground became exposed. Q* was greater, and more often positive, at Nier. As before, downward H closely matched upward λE at both BV and Nier; the magnitude of turbulent fluxes were greater at BV (Fig. 7). Snowcover remained complete at BV during this chinook but became damp from early 25 January, whereas the snowcover became patchy and damp at Nier by 23 January. The magnitudes of turbulent fluxes at BV were similar during the initial cold period with blowing snow as they were during the period with a damp and static snowpack (e.g. 10–100 W m^{-2}), whereas the fluxes were larger at Nier when the snowpack was wet and patchy (often exceeding 80 W m^{-2} compared to under 20 W m^{-2} during cold period). The largest turbulent fluxes at both BV and Nier corresponded with higher u*, air temperature and VPD. G remained low at both sites, but reached maximum downward values of approximately 50 W m^{-2} during positive Q* at Nier. Average daily evaporation + sublimation during this chinook was 1.54 mm/day at BV and 0.93 mm/day at Nier,

Time-lapse photographs show that initially there was only a trace amount of snowcover at Lethbridge. The area was snow-free by the morning of 22 January but remained damp. The surface was dry by 23 January. λE fluxes were much smaller at Lethbridge than at BV or Nier. Mean λE was 8.5 W m^{-2} and 3.5 W m^{-2} during the damp and dry periods, respectively, and maximum λE was 29.7 W m^{-2} and 15.9 W m^{-2} during the damp and dry periods, respectively. H fluxes were of similar mean value as at BV and Nier, though there were both large positive and negatives fluxes (maximum of 90.5 W m^{-2} and minimum of −128 W m^{-2}). At Lethbridge, upward H was again associated with periods of positive Q* during daytime. Peaks in positive λE at Lethbridge occurred with positive Q*. G remained low (± 20 W m^{-2}) at Lethbridge. Average daily evaporation + sublimation during this chinook was 0.14 mm/day at Lethbridge.

With respect to soil temperatures and LWC, the most notable difference from the 4–6 December chinook was that soil temperatures were now below freezing at Lethbridge (not shown). Again, soil temperatures varied diurnally according to positive Q*, and generally increased throughout the chinook.

3.1.3. 6–15 March 2012

Again there was a spatial progression resulting in a temporal lag in chinook occurrence amongst sites, with increasing u*, air temperature and VPD occurring approximately 7 h later and less rapidly at Nier than at BV and Lethbridge (Fig. 8).

Initially, there was a deep snowpack at BV, and half this depth at Nier (Fig. 9). Blowing snow occurred at BV and Nier until early 8 March, eroding about 3.0 cm and 3.7 cm of snow depth respectively. Snowcover became wet and patchy at BV and Nier by 8 March and disappeared entirely by 10 March at BV and 11 March at Nier. The surface remained damp at BV until a small overnight snowfall event on 11–12 March. The snow was completely removed by wind and snowmelt by midday 12 March. There was another brief snowfall event on 13 March at both BV and Nier. Blowing snow occurred at BV, followed by melt resulting in a bare yet damp surface by 14 March until the end of 15 March. There was less snowfall at Nier and air temperatures were 5–10 °C higher than at BV, so the snowpack was likely removed via melt by 14 March.

The magnitude of turbulent fluxes was again greater at BV than at Nier throughout the chinook (Fig. 9). There were three periods with cold temperatures and blowing snow at BV and two periods at Nier. The magnitudes of fluxes were largest during wet and patchy snowcovers, exceeding 80 W m^{-2} and reaching 200 W m^{-2} at BV. Latent heat fluxes were similar during bare and damp conditions as during colder periods with blowing snow. Again, downward H matched upward λE at both BV and Nier. Q* was much higher during this chinook compared to the others due to greater solar irradiance and lesser snow coverage. As opposed to the previous chinook events, upward H driven by Q* was observed at both BV and Nier as snow disappeared from 10 March onwards. It appears that high positive Q* drove upward λE at times at both BV and Nier (e.g. 12 and 14 March). Average daily evaporation + sublimation during this chinook was 2.08 mm/day at BV and 0.88 mm/day at Nier.

Time-lapse photography at Lethbridge initially showed a trace amount of patchy snowcover, which disappeared entirely during 7 March. The surface was bare and dry from 8 March. Again, Q* was driving small upward λE. Average daily evaporation + sublimation during this chinook was 0.08 mm/day at Lethbridge.

It is during this chinook that infiltration and soil temperatures above freezing were first observed after winter. Points labelled VWC (volumetric water content) in Fig. 10 indicate when soils were completely unfrozen and reliable measures of total volumetric water content were possible. A soil temperature of 0 °C was used as the limit above which soils were considered completely unfrozen. This limit was established by examining soil temperature time series, and was set high to avoid erroneously attributing soil VWC changes to those resulting from phase change. Again, soil temperatures and LWC were greatest at Lethbridge. LWC at Lethbridge increased generally throughout the chinook, mostly due to phase change as surface water was not available for infiltration except during 6–7 March. Increasing soil moisture through 8 March at BV was mostly due to soil thaw, and this was the case through mid-day 10 March at Nier. Soil temperatures increased sharply and were well above freezing during the days of 10 and 11

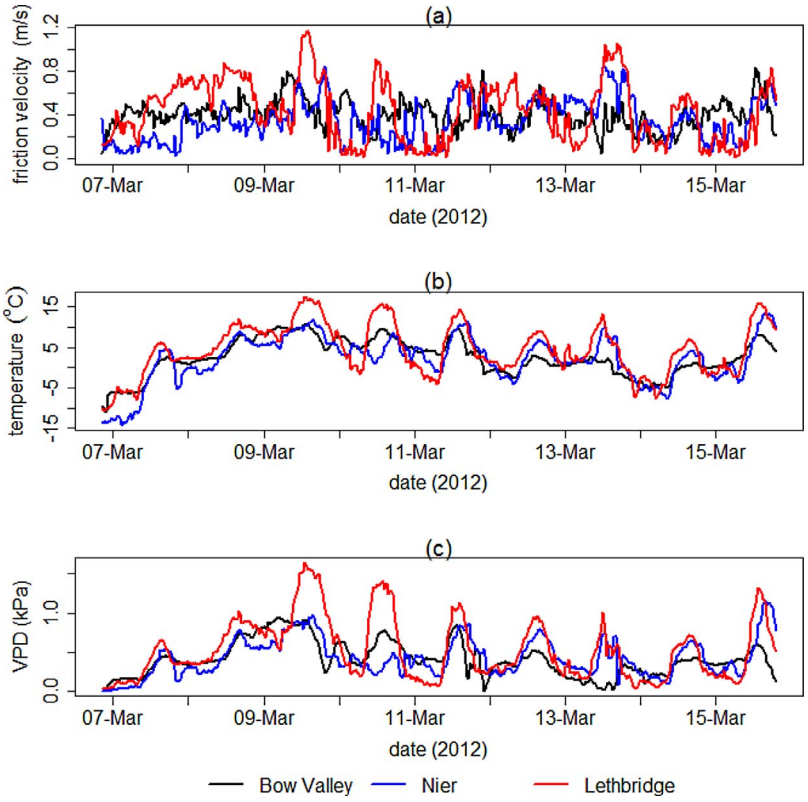

Fig. 8. Surface meteorology at all sites for 6–15 March 2012: (a) friction velocity (u*), (b) air temperature, and (c) vapour pressure deficit.

March at both BV and Nier, coincident with high Q* and downward G. It's unclear if increasing soil moisture at 2 cm (BV) and 5 cm (Nier) during these periods was due to phase change or infiltration, as temperatures were well above freezing and the max LWC calculation was not applicable.

3.1.4. Discussion

The observations highlight differences in responses to chinooks during snow-covered versus snow-free periods and low versus high solar radiation periods. Snowcovers did not disappear completely at BV or Nier during the winter chinooks (4–6 December and 21–26 January) and upward λE was driven by downward H. Snowcovers disappeared entirely at BV and Nier during the spring chinook (6–15 March) and solar irradiance was greater. As a result, Q* was greatest during the spring chinook. This resulted in a shift to upwards H during the day while Q* was positive. Averaged over all sites and surface conditions, the mean magnitude of H was greater (i.e. more downward) during low Q* periods than during high Q* periods (-42.6 W/m^2 vs -11.2 W/m^2). Despite the shift in the direction of H, the mean magnitudes of upward λE were approximately the same during the winter and spring chinooks (30.6 W/m^2 during low Q* and 32.9 W/m^2 during high Q*).

The time series from the three select events show the progression of chinooks from an initial cold period with complete snowcovers (if present) to potentially fully exposed and dry surfaces.

3.1.4.1. Initial cold period with complete snow cover (if present). This period spans the onset of chinook while air temperatures are mostly below freezing, up until snowpacks become warm and contain significant liquid water. Snow redistribution by wind and sublimation enhanced by blowing snow occur. Upward λE is driven by downward H. This period was observed at both BV and Nier from the beginning of all three select chinooks. For the March chinook there were three instances of this period at BV due to breaks in the chinooks and snowfall occurring. The greatest loss of snow depth occurred during this period.

3.1.4.2. Wet snowpacks becoming patchy. This period is characterised by shallow snowcovers becoming patchy with high liquid water content and high sublimation and evaporation rates. Blowing snow has ceased. Upward λE is driven by downward H. This period was observed at both BV and Nier during each of the three chinooks. For the December and January events this period occurred from the end of the initial cold period until the cessation of the chinook. For the March event this period preceded complete disappearance of the snowpack at BV and Nier. This period occurred for only a brief time at Lethbridge (i.e. a few hours) as there were only a trace depth of snow. The largest turbulent fluxes occurred during this period. The fluxes averaged over both BV and Nier for all three events give mean $H = -68.4\ W\ m^{-2}$ and $\lambda E = 84.3\ W\ m^{-2}$, as opposed to mean $H = -45.9\ W\ m^{-2}$ and $\lambda E = 46.7\ W\ m^{-2}$ during the initial cold period with blowing snow. It is noted, however, that not all sublimation of blowing snow was measured by the KH2O krypton hygrometer as some particle transport occurs at elevations above those which are measured by the device.

3.1.4.3. Largely snowfree surface with some surface water. This period was characterised by damp and exposed ground undergoing evaporation. This period occurred at BV and Nier only during the March event: three times at BV and twice at Nier. This period occurred at Lethbridge during each of the select chinooks.

3.1.4.4. Snowfree and mostly dry surface. This period occurred only at Lethbridge. Evaporation rates are low and sensible heat fluxes are positive as a result of higher downward Q*.

3.2. Seasonal water balance

Winter water balance components are assessed from 1 November 2011 for BV and Lethbridge, but from only 3 December 2011 for Nier due to the availability of flux observations (Fig. 11 and Table 7). SWE was considerably lower than cumulative precipitation at both BV and Nier, with alternating increasing and decreasing SWE as snow fell

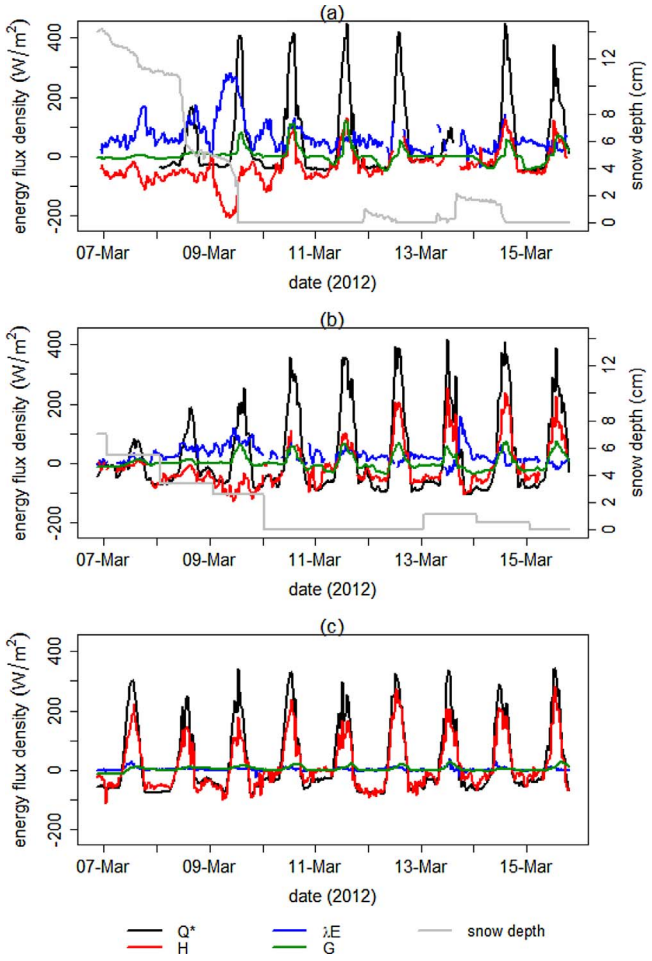

Fig. 9. Energy fluxes and snow depth for 6–15 March 2012 at (a) Bow Valley, (b) Nier, and (c) Lethbridge. Snow depth is not shown for Lethbridge because only a trace amount was initially present and measurements were degraded by vegetation.

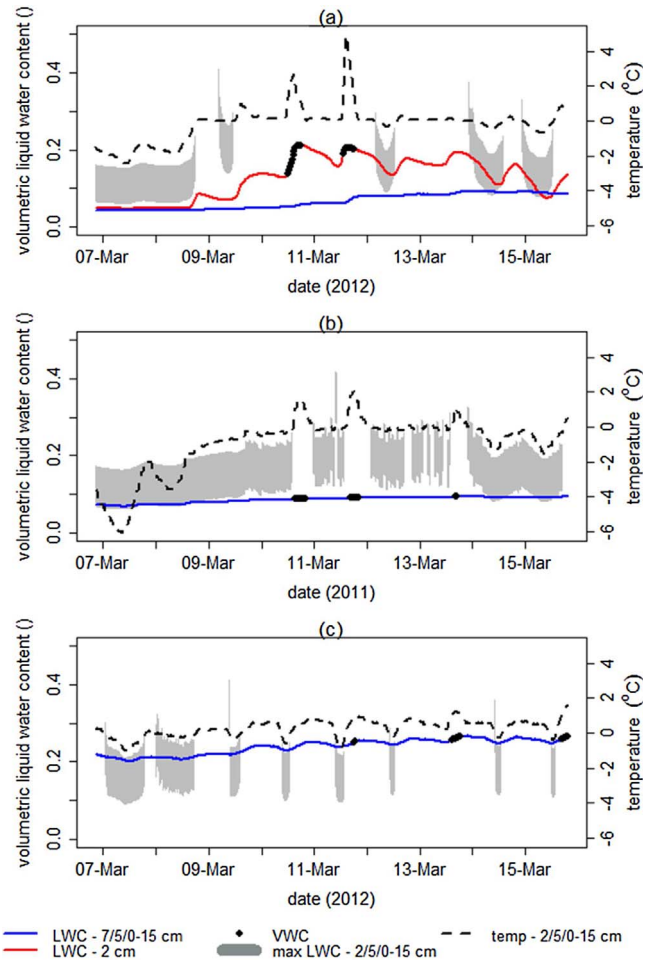

Fig. 10. Soil temperature, observed unfrozen water content and calculated maximum unfrozen water content for 6–15 March 2012 at (a) Bow Valley, (b) Nier, and (c) Lethbridge. The range in calculated maximum in LWC is calculated using mean hydraulic parameter values ± 1 standard deviation.

between chinooks and was ablated during chinooks. Cumulative E (evaporation + sublimation) was near the lower bound of cumulative precipitation at both BV and Nier by early April. Cumulative E at BV was double that at Nier, matching the approximate double precipitation at BV relative to Nier, and approximately seven times that at Lethbridge.

Over the study period there were increases of 7.4 mm to 8.5 mm of soil water at BV and 1.8–2.0 mm at Nier, and a decrease of 4.1–5.6 mm at Lethbridge (Table 7). During November, VWC decreased at all depths at BV and Lethbridge, indicating soil water evaporation, whereas soils remained most often frozen at Nier (Fig. 12). Soils to 20 cm remained partially frozen from mid-November through late-March. Soil water content at BV and Nier increased over winter, but decreased at Lethbridge. It is likely that there was little evaporation of existing soil moisture at any of the sites while soils were frozen from December through March, and that most of the upward water vapour fluxes were from snowpacks and meltwater. This is corroborated by the times series of observed and theoretical maximum LWC indicating that increasing soil water was mostly due to phase change (Figs. 5 and 10).

For water balance closure at the experimental sites there should be correspondence between observed and calculated ΔS in Table 7. There was not a consistent water balance closure across all sites for any particular source of precipitation data. At BV, the observed increase in ΔS corresponded best using CaPA precipitation but was slightly underestimated using the nearby gauge data. At Nier, both reanalyses resulted in calculated ΔS that compared favourably with observed ΔS but gauge data resulted in slightly overestimating the observed ΔS (by 6.0 mm). At Lethbridge, the observed decrease in ΔS was overestimated with all sources of precipitation data. No snow transport was simulated or observed at this site.

4. Synthesis of energy and water balances

Synthesizing results from the time series analyses and seasonal water balances provides insight into the controlling factors and spatiotemporal variability of energy and water fluxes as affected by chinooks.

Observations indicate that snowfall and the presence of snowcover were the principal factors controlling inter-site differences in energy and water fluxes. The energy balance time series showed that downward H during chinooks was driving upward λE when snowcover was present; this occurred at the snow-heavy BV and Nier sites. Conversely, the energy balance time series at the frequently snow-free Lethbridge site showed that positive Q* was driving upward λE. Upward H fluxes were observed frequently at Lethbridge as opposed to BV and Nier; surface water availability was lower at Lethbridge so less energy was directed towards evaporation. Similarly, upward H fluxes during March were greater in magnitude at Nier, where snow was not present, than at BV. Ratios of cumulative E to CaPA precipitation were similar at BV (0.84–0.93) and Nier (0.90–0.99); this calculation was not performed for Lethbridge due to poor water balance closure.

Observed daily E during the select chinooks were generally higher at BV than at Nier and much higher than at Lethbridge. These daily E at

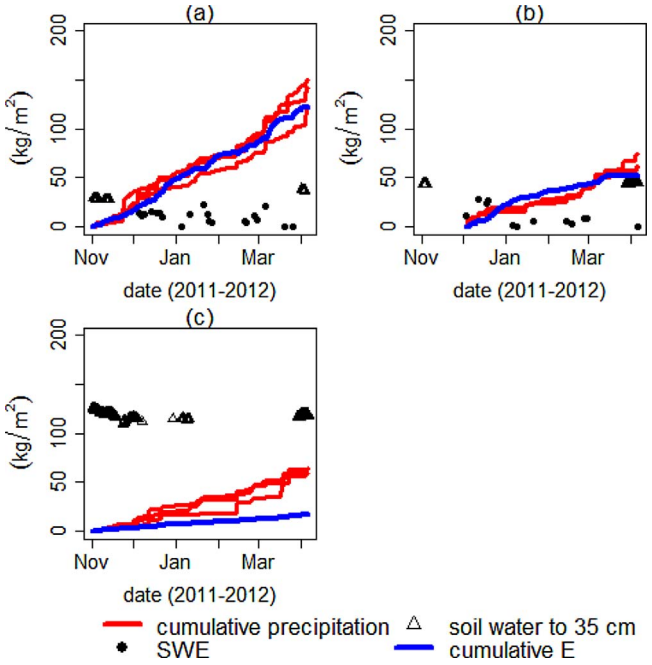

Fig. 11. Winter water balance components at (a) Bow Valley, (b) Nier, and (c) Lethbridge.

BV and Nier, ranging from 0.93 mm/day to 2.08 mm/day (1.0 mm/day to 2.3 mm/day if E was underestimated by 10%), are comparable to values from other studies. The daily E rates at BV were consistent with those from a nearby mountainous site during the 1970s (1.2–2.0 mm/day (Golding, 1978)). They are similar to daily fluxes during chinooks in alpine regions of the western USA (over 2 mm/day (Cline, 1997), 0.5 mm/day (Hood et al., 1999)). The daily E fluxes are also similar to observations during foehn in Japan (Hayashi et al., 2005); however they are higher than the continuous snowcover sublimation fluxes measured by Granger and Male (1978) 500 km east and away from the frequent chinook zone by at least an order of magnitude.

The energy balance non-closure shown in Table 3 affects the strength of these conclusions. The non-closure implies either underestimated turbulent fluxes (i.e. greater evaporation or sublimation, missing blowing snow sublimation or downward H) or missed phase change, during which meltwater would have refrozen following the cessation of chinooks. Lethbridge had the best energy balance closure, but worst water balance closure across the sites. It's conceivable that upward missed upward λE could account for this non-closure at Lethbridge; however, there is no indication that latent heat fluxes at Lethbridge should be nearly as high as those at BV and Nier e.g. little winter precipitation. It is plausible that the instrumentation missed several smaller magnitude turbulent at all sites, particular during stable conditions. It is noted that the magnitude of energy balance residuals in Table 3 are of similar magnitudes to the period-average measured fluxes in Table 5. Therefore, the state evaporation estimate are not without error, but the relative site differences in fluxes are reasonable given differences in water availability, wind speed, humidity and Q*. Energy balance closure over complex terrain and snowcovers remains an outstanding issue and should remain an active area of research, such as those pursued by Helgason and Pomeroy (2012a,b) among others.

5. Conclusions

Detailed observations from three prairie sites in southern Alberta over winter 2011–2012 were used to characterise the spatial and seasonal variability of water and energy fluxes during chinooks. Time series of select chinook events were examined and the observed water balances were assessed.

The temporal progression of chinooks was identified. Initially air temperatures remain cold and most snow mass in open areas, if substantial, is removed as blowing snow. Air temperatures then rise and the remaining snowpacks melt and become patchy. The largest turbulent fluxes occurred during this period. Evaporation of surface water can continue after snowpacks disappear entirely.

Snowcover played a strong role in regulating spatial differences in energy balances. The largest upward latent heat fluxes occurred at BV where winter precipitation was greatest. The smallest fluxes occurred where there was little winter precipitation, at the southernmost Lethbridge site, even though soil water content was much greater at this site. During winter chinooks, large upward latent heat fluxes were largely caused by downward sensible heat fluxes at the two sites with greater snowfall, longer snow-covered period and greater blowing snow potential (BV and Nier). Conversely, at the relatively snow-free Lethbridge, the largest upward latent heat fluxes were caused by positive net radiation which also resulted in upward sensible heat fluxes. It was not until spring that upward sensible heat fluxes driven by positive net radiation were observed at BV and Nier. Flux measurements in complex terrain, particularly over snowcovers or during stable conditions, remain an outstanding challenge. The non-closure confounds the accuracy of measurements presented in this paper.

Observations indicate some soil water evaporation during November, but little soil water evaporation during winter. There was no evidence of infiltration during winter; rather, soil liquid water content changes occurred mostly as a result of freezing and thawing. Recent precipitation supplied nearly all upward vapour fluxes during winter. Soil water storage increases over winter were small at these open sites. Cumulative winter precipitation of over 145 mm (CaPA) at BV resulted in only a 7.4 mm to 8.5 mm increase in storage. Cumulative winter precipitation of 57 mm (CaPA) at Nier resulted in only a 1.8 mm to 2.0 mm increase in sub-surface storage. These storage observations do not account for the likely greater increases in storage at other locations due to snow redistributed by wind from the experimental sites.

Table 7
Observed and estimated water balance components from 1 November 2011–3 April 2012 (Bow Valley and Lethbridge) and from 3 December 2011–3 April 2012 (Nier). Q_T is snow transport by wind away from the site, which estimated using PBSM/EBSM. All values in kg m^{-2}.

Site	P	E	Q_T	Observed ΔS	Calculated ΔS
Bow Valley	129.4 (Bow Valley)	122.2–134.4	1.4–6.4	7.4–8.5	−11.4 to 5.8
	144.9 (CaPA)		8.2–8.5		2.0–14.5
	103.9 (ERA-interim)		0.9–5.9		−36.4 to −19.2
Nier	67.6 (Nier)	51.7–56.9	1.5–2.7	1.8–2.0	8.0–14.4
	57.2 (CaPA)		0.02–1.7		−1.4 to 5.5
	55.9 (ERA-interim)		0.03–2.4		−3.4 to 4.2
Lethbridge	56.8 (Demo Farm)	17.1–18.8	0	−5.6 to −4.1	38.0–39.7
	63.6 (CaPA)		0		44.8–46.5
	58.9 (ERA-interim)		0		40.1–41.8

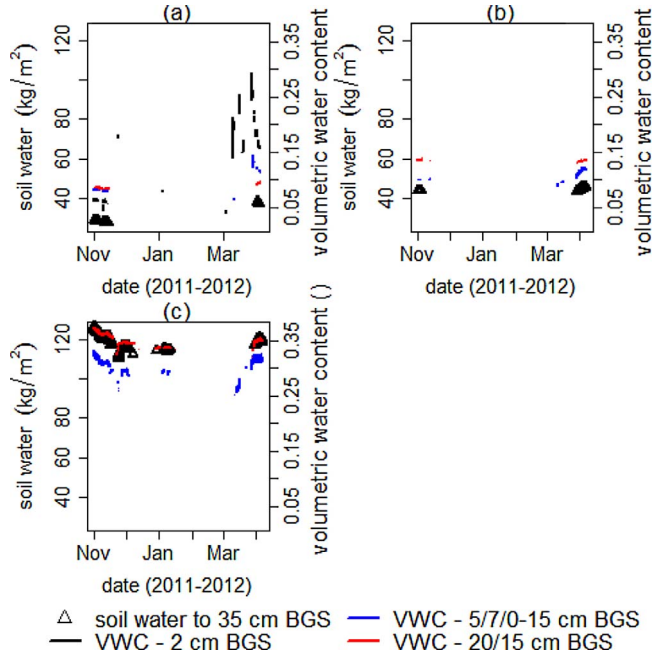

Fig. 12. Winter soil water balance components at (a) Bow Valley, (b) Nier, and (c) Lethbridge.

Acknowledgments

This research was supported by the Canada Research Chairs Programme, Alberta Department of Agriculture and Forestry, Natural Sciences and Engineering Research Council of Canada, European Space Agency and the University of Edinburgh School of GeoSciences. Data from the Lethbridge site was provided by L.B. Flanagan (University of Lethbridge) from a research program funded by the Natural Sciences and Engineering Research Council of Canada. The authors extend gratitude to L.B. Flanagan, and Ralph Wright and Dave Clarke (Alberta Agriculture and Rural Development) for allowing instrument installation, providing logistical support, and sharing data for the Lethbridge site and Nier site, respectively. Robert Clement (University of Edinburgh) provided guidance on flux correction. May Guan (University of Saskatchewan) assisted with instrument deployment.

References

American Meteorological Society (AMS), 2012. Glossary of Meteorology. Accessed 30 April 2016. http://glossary.ametsoc.org/wiki/Chinook.
Black, P.D., Tice, R.A., 1988. Comparison of soil freezing curve and soil water curve data for windsor sandy loam. US Army Cold Reg. Res. Eng. Rep. 88–116.
Chen, N., Guan, D., Jin, C., Wang, A., Wu, J., Yuan, F., 2011. Influences of snow event on energy balance over temperate meadow in dormant season based on eddy covariance measurements. J. Hydrol. 399, 100–107.
Clapp, R., Hornberger, G., 1978. Empirical equations for some soil hydraulic properties. Water Resour. Res. 14, 601–604.
Cline, D.W., 1997. Snow surface energy exchanges and snowmelt at a continental mid-latitude Alpine site. Water Resour. Res. 33, 689–701.
Constantin, J., Inclan, M.G., Raschendorfer, M., 1998. The energy budget of a spruce forest: field measurements and comparison with the forest-land-atmosphere model (FLAME). J. Hydrol. 213, 22–35.
Cosby, B.J., Hornberger, G.M., Clapp, R.B., Ginn, T.R., 1984. A statistical exploration of the relationships of soil moisture characteristics to the physical properties of soils. Water Resour. Res. 20, 682–690.
Dee, D.P., Uppala, S.M., Simmons, A.J., Berrisford, P., Poli, P., Kobayashi, S., Andrae, U., Balmaseda, M.A., Balsamo, G., Bauer, P., Bechtold, P., Beljaars, A.C.M., van de Berg, L., Bidlot, J., Bormann, N., Delsol, C., Dragani, R., Fuentes, M., Geer, A.J., Haimberger, L., Healy, S.B., Hersbach, H., Hólm, E.V., Isaksen, L., Kållberg, P., Köhler, M., Matricardi, M., McNally, A.P., Monge-Sanz, B.M., Morcrette, J.-J., Park, B.-K., Peubey, C., de Rosnay, P., Tavolato, C., Thépaut, J.-N., Vitart, F., 2011. The ERA-Interim reanalysis: configuration and performance of the data assimilation system. Q. J. R. Meteorolog. Soc. 137, 553–597.
Famiglietti, J.S., Dongryeol, R., Berg, A.A., Rodell, M., Jackson, T.J., 2008. Field observations of soil moisture variability across scales. Water Resour. Res. 44, W01423.
Fang, X.F., Pomeroy, J.W., 2009. Modelling blowing snow redistribution to prairie wetlands. Hydrol. Process. 23, 2557–2569.
Fang, X.F., Pomeroy, J.W., Ellis, C.R., MacDonald, M.K., DeBeer, C.M., 2013. Multi-variable evaluation of hydrological model predictions for a headwater basin in the Canadian Rocky Mountains. Hydrol. Earth Syst. Sci. 17, 1635–1659.
Flanagan, L.B., Adkinson, A.C., 2011. Interacting controls on productivity in a northern Great Plains grassland and implications for response to ENSO events. Glob. Change Biol. 17, 3293–3311.
Flanagan, L.B., Wever, L.A., Carlson, P.J., 2002. Seasonal and interannual variation in carbon dioxide exchange and carbon balance in a northern temperate grassland. Glob. Change Biol. 8, 599–615.
Flerchinger, G.N., Saxton, K.E., 1989. Simultaneous heat and water model of a freezing snow-residue-soil system I. Theory and development. Trans. AS AE 32, 565–571.
Foken, T., Wichura, B., 1996. Tools for quality assessment of surface-based flux measurements. Agric. For. Meteorol. 78, 83–105.
Foken, T., 2008. Experimental methods for estimating the fluxes of energy and matter: eddy-covariance method. In: Foken, T., Nappo, C.J. (Eds.), Micrometeorology. Springer, Berlin, pp. 105–122.
Fuchs, M., Campbell, G.S., Papendick, R.I., 1978. An analysis of sensible and latent heat flow in a partially frozen unsaturated soil. Soil Sci. Soc. Am. 42, 379–385.
Golding, D.L., 1978. Calculated snowpack evaporation during Chinooks along the eastern slopes of the Rocky Mountains in Alberta. J. Appl. Meteorol. 17, 1647–1651.
Granger, R.J., Male, D.H., 1978. Melting of a Prairie Snowpack. J. Appl. Meteorol. 17, 1833–1842.
Gray, D.M., Landine, P.G., 1988. An energy-budget snowmelt model for the Canadian Prairies. Can. J. Earth Sci. 25, 1292–1303.
Gray, D.M., Granger, R.J., Dyck, G.E., 1985a. Overwinter soil moisture changes. Trans. Am. Soc. Agric. Eng. 28, 442–447.
Gray, D.M., Landine, P.G., Granger, R.J., 1985b. Simulating infiltration into frozen prairie soils in streamflow models. Can. J. Earth Sci. 22, 464–472.
Gray, D.M., Pomeroy, J.W., Granger, R.J., 1986. Prairie snowmelt runoff. In: Proceedings, Water Research Themes, Conference Commemorating the Official Opening of the National Hydrology Research Centre. Saskatoon, SK. pp. 49–68.
Haslwanter, A., Hammerle, A., Wohlfahrt, G., 2009. Open- vs. closed-path eddy covariance measurements of the net ecosystem carbon dioxide and water vapour exchange: a long-term perspective. Agric. For. Meteorol. 149, 291–302.
Hayashi, M., Hirota, T., Iwata, Y., Takayabu, I., 2005. Snowmelt energy balance and its relation to foehn events in Tokachi, Japan. J. Meteorol. Soc. Japn. 83, 783–798.
Helgason, W.D., Pomeroy, J.W., 2012a. Problems closing the energy balance over a homogeneous snow cover during midwinter. J. Hydrometeorol. 13, 557–572.
Helgason, W.D., Pomeroy, J.W., 2012b. Characteristics of the near-surface boundary layer within a mountain valley during winter. J. Appl. Meteorol. 51, 583–597.
Hood, E., Williams, M., Cline, D., 1999. Sublimation from a seasonal snowpack at a continental mid-latitude alpine site. Hydrol. Process. 13, 689–704.
Kaimal, J.C., Wyngaard, J.C., Izumi, Y., Cote, O.R., 1972. Spectral characteristics of surface-layer turbulence. Q. J. R. Meteorol. Soc. 98, 563–589.
Kaimal, J.C., Wyngaard, J.C., Haugen, D.A., Cote, O.R., Izumi, Y., Caughey, S.J., Readings, C.J., 1976. Turbulence structure in the convective boundary layer. J. Atmos. Sci. 33, 2152–2169.
Kelliher, F.M., Hollinger, D.Y., Schulze, E.D., Vygodskaya, N.N., Byers, J.N., Hunt, J.E., McSeveny, T.M., Milukova, I., Sogatchev, A., Varlargin, A., Ziegler, W., Arneth, A., Bauer, G., 1997. Evaporation from an eastern Siberian larch forest. Agric. For. Meteorol. 85, 135–147.
Leuning, R., van Gorsel, E., Massman, W.J., Isaac, P.R., 2012. Reflections on the surface energy imbalance problem. Agric. For. Meteorol. 156, 65–74.
Leydecker, A., Melack, J.M., 1999. Evaporation from snow in the central Sierra Nevada of California. Nordic Hydrol. 30, 81–108.
Li, L., Pomeroy, J.W., 1997. Probability of occurrence of blowing snow. J. Geophys. Res. D: Atmos. D18, 21955–21964.
Mahfouf, J.-F., Basnett, B., Gagnon, S., 2007. A Canadian precipitation analysis (CaPA) project: Description and preliminary results. Atmos. Ocean 45, 1–17.
Mauder, M., Liebethal, C., Göckede, M., Leps, J.-P., Beyrich, F., Foken, T., 2006. Processing and quality control of flux data during LITFASS-2003. Boundary Layer Meteorol. 121, 67–88.
Miller, R., 1965. Phase equilibria and soil freezing. In: Proc. Second Int. Conf. National Research Council Publication, National Academy of Sciences, Washington, DC. pp. 193–197.
Moore, C.J., 1986. Frequency response corrections for eddy correlation systems. Boundary Layer Meteorol. 37, 17–35.
Musselman, K.N., Pomeroy, J.W., Essery, R.L.H., Leroux, N., 2015. Impact of windflow calculations on simulations of alpine snow accumulation, redistribution and ablation. Hydrol. Process. 29, 3983–3999.
Nkemdirim, L.C., 1991. Chinooks and winter evaporation. Theor. Appl. Climatol. 43, 129–136.
Nkemdirim, L.C., 1996. Canada's chinook belt. Int. J. Climatol. 16, 441–462.
Nkemdirim, L.C., 1997. On the frequency and sequencing of Chinooks. Phys. Geogr. 18, 101–113.
Ohta, T., Hiyama, T., Tanaka, H., Kuwada, T., Maximov, T.C., Ohata, T., Fukushima, Y., 2001. Seasonal variation in the energy and water exchanges above and below a larch forest in eastern Siberia. Hydrol. Process. 15, 1459–1476.
Pomeroy, J.W., Essery, R.L.H., 1999. Turbulent fluxes during blowing snow: field tests of model sublimation predictions. Hydrol. Process. 13, 2963–2975.
Pomeroy, J.W., Gray, D.M., 1995. Estimating blowing snow transport and sublimation rates on the prairies of Western Canada. In: Pomeroy, J.W., Gray, D.M. (Eds.), Snowcover Accumulation, Relocation and Management. National Hydrology Research Institute Science Report No. 7, Saskatoon,Saskatchewan, Canada, pp.

79–98.
Pomeroy, J.W., Li, L., 2000. Prairie and arctic areal snow cover mass balance using a blowing snow model. J. Geophys. Res. Atmos. 105, 26619–26634.
Pomeroy, J.W., Gray, D.M., Landine, P.G., 1993. The prairie blowing snow model: characteristics, validation, operation. J. Hydrol. 144, 165–192.
Richardson, A.D., Jenkins, J.P., Braswell, B.H., Hollinger, D.Y., Ollinger, S.V., Smith, M.-L., 2007. Use of digital webcam images to track spring green-up in a deciduous broadleaf forest. Oecologia 152, 323–334.
Smith, C.D., 2009. The relationship between snowfall catch efficiency and wind speed for the Geonor T-200 B precipitation gauge utilizing various wind shield configurations. In: Proc 2009 Western Snow Conference. Canmore, Alberta, Canada. pp. 115–121.
Soil Landscapes of Canada Working Group, 2010. Soil Landscapes of Canada Version 3.2 (digital Map and Database at 1:1 Million Scale). Agriculture and Agri-Food Canada. Accessed 16 May 2013. http://sis.agr.gc.ca/cansis/nsdb/slc/v3.2/index.html.
Steed, G.L., 1982. The effect of cover and chinooks on snowpack in Alberta. Proc. Can. Hydrol. Symp. 138–146.
Vickers, D., Mahrt, L., 1997. Quality control and flux sampling problems for tower and aircraft data. J. Atmos. Oceanic Technol. 14, 512–526.
Webb, B.W., Pearman, G.I., Leuning, R., 1980. Correction of flux measurements for density effects due to heat and water vapour transfer. Q. J. R. Meteorol. Soc. 106, 85–100.
Wilczak, J.M., Oncley, S.P., Stage, S.A., 2001. Sonic anemometer tilt correction algorithms. Boundary Layer Meteorol. 99, 127–150.
Wilson, K., Goldstein, A., Falge, E., Aubinet, M., Baldocchi, D., Berbigier, P., Bernhofer, C., Ceulemans, R., Dolman, H., Field, C., Grelle, A., Ibrom, A., Law, B.E., Kowalski, A., Meyers, T., Moncrieff, J., Monson, R., Oechel, W., Tenhunen, J., Valentini, R., Verma, S., 2002. Energy balance closure at FLUXNET sites. Agric. For. Meteorol. 113, 223–243.
Zhao, L., Gray, D.M., 1997. A parametric expression for estimating infiltration into frozen soils. Hydrol. Process. 11, 1767–1775.